Hindawi
Modelling and Simulation in Engineering
Volume 2020, Article ID 5046286, 11 pages
https://doi.org/10.1155/2020/5046286

Research Article

Noniterative Localized and Space-Time Localized RBF Meshless Method to Solve the Ill-Posed and Inverse Problem

Mohammed Hamaidi,[1] Ahmed Naji,[1] Fatima Ghafrani,[2] and Mostafa Jourhmane[3]

[1]*Department of Mathematics, Faculty of Sciences and Techniques, Abdelmalek Essaadi University, Box 416, Tangier, Morocco*
[2]*Department of Mathematics, Polydisciplinary Faculty of Larache, Abdelmalek Essaadi University, Box 745, Larache, Morocco*
[3]*Department of Mathematics, Faculty of Sciences and Techniques, University of Sultan Moulay Slimane, Box 523, Beni Mellal, Morocco*

Correspondence should be addressed to Mohammed Hamaidi; hamaidi@yahoo.com

Received 17 September 2019; Revised 30 April 2020; Accepted 15 May 2020; Published 17 June 2020

Academic Editor: Jean-Michel Bergheau

In many references, both the ill-posed and inverse boundary value problems are solved iteratively. The iterative procedures are based on firstly converting the problem into a well-posed one by assuming the missing boundary values. Then, the problem is solved by using either a developed numerical algorithm or a conventional optimization scheme. The convergence of the technique is achieved when the approximated solution is well compared to the unused data. In the present paper, we present a different way to solve an ill-posed problem by applying the localized and space-time localized radial basis function collocation method depending on the problem considered and avoiding the iterative procedure. We demonstrate that the solution of certain ill-posed and inverse problems can be accomplished without iterations. Three different problems have been investigated: problems with missing boundary condition and internal data, problems with overspecified boundary condition, and backward heat conduction problem (BHCP). It has been demonstrated that the presented method is efficient and accurate and overcomes the stability analysis that is required in iterative techniques.

1. Introduction

In contrast to the stationary and nonstationary direct boundary value problems, ill-posed problems are characterized by unknown boundary conditions on a part of the boundary. An example is the problem of determining the temperature and the heat flux on the whole boundary or on its part, where the temperature and the heat flux are prescribed in selected points located inside the domain of the considered problem. Another statement of ill-posed problems is the one referred to as the final boundary value problem or backward heat conduction problem (BHCP). The problem is characterized by the unknown initial condition value. The temperature distribution and the heat flux are investigated from the known data which can be the temperature distribution at particular time $t = t_f > 0$. From this data, the question arises as to whether the temperature distribution at any earlier time $t < t_f$ can be retrieved.

Since the solution of the BHCPs does not continuously depend on the given final data, it shows some difficulties to be solved using classical methods. So, many iterative schemes have been developed during the last decade. Some of them have been proposed by Kozlov and Maz'ya [1], Mera et al. [2], and Jourhmane et al. [3]. Some other methods based on the BEM, regularization techniques, and FSM cited in [4–9] are applied. For recently developed methods, we can mention the work developed by Ma et al. [10]. They transform the problem into an optimization one and use a conjugate gradient method to solve the inverse problem.

The investigations of the meshless method based on radial basis functions (RBFs) have seen many developments. For BHCP, we can mention the meshless method developed by Li et al. [11] based on the RBF method for the nonhomogeneous backward heat conduction problem. Beside the first work done by Cheng and Cabral [12] using global RBF to solve Poisson problems, we can cite the recent work published

by Li et al. [13] in which they presented a stable local meshless collocation method based on CS-RBFs for solving certain inverse problems. Gu et al. [14] have also proposed a meshless singular boundary method for three-dimensional inverse heat conduction problems in general anisotropic media. Wang et al. introduced a stable and accurate meshless method based on collocation and radial basis functions to solve the inverse wave problem [15]. Compared to other methods, no iterative algorithm is needed in their new developed method. Furthermore, they addressed their noniterative method to identify the initial conditions [16] and boundary condition [17] arising in the inverse wave problem.

In this paper, a local mesh-free method based on RBFs for solving ill-posed problems was presented. For the first case, we solve a Poisson problem in the two-dimensional domain with missing boundary conditions in a part of the boundary. The two types of examples considered are a problem with missing boundary condition and internal data and a problem with overspecified boundary condition. And for the second case, we solve a nonstationary backward heat conduction problem (BHCP) characterized by the final condition using the space-time localized RBF collocation method. The technique is based on transforming the parabolic system from a d-dimensional problem into a $(d+1)$-dimensional one without distinguishing between the space and time variables. The collocation points have both the space and time coordinates. The (BHCP) parabolic equation is then solved by using the governing domain equation as condition on the boundary of missing condition, characterized by $\{t=0\}$ for BHCP. An advanced feature of our approach is that we solve the problem in one step for the tree treated examples without any iterative scheme. Another novelty is to use the space-time approach for (BHCP)example and no time integration method is used. The present method is expected to be free of disadvantages related to the loss of stability of solutions due to the iteration schemes. In our approach, the problem is considered a well-posed one and the algebraic system solved is square for all cases. Results of numerical simulations given in the present paper show that the method is stable and efficient. Note that the two-dimensional nonstationary problems can be solved using the same approach.

2. Mathematical Formulation of the Problems

In this section, we give a brief description of the models of the ill-posed boundary value problem considered in this work. The first treated problem, characterized by missing boundary condition and internal data, has the following form:

$$\begin{cases} \Delta u(x,y) = f(x,y), & (x,y) \in \Omega = \left]0, \ell_x\right[\times\left]0, \ell_y\right[, \\ u(x,0) = g_2(x), & x \in [0, \ell_x], \\ u(0,y) = h_1(y), & y \in \left]0, \ell_y\right], \\ u(\ell_x, y) = h_2(y), & y \in \left]0, \ell_y\right], \\ u(x, \ell_{\text{int}}) = g_1(x), & x \in \left]0, \ell_x\right[. \end{cases} \tag{1}$$

The internal data for this problem is described by $u(x, \ell_{\text{int}}) = g_1(x)$with $\ell_{\text{int}} < \ell_y$ and $x \in \left]0, \ell_x\right[$. No boundary condition is taken on the fourth side $\{y = \ell_y\,; 0 < x < \ell_x\}$. Figure 1 describes the domain considered with the boundary and internal conditions.

The second problem is a stationary heat problem with missing boundary condition and overspecified boundary condition on one part of the boundary; this problem has the following form:

$$\begin{cases} \Delta u(x,y) = f(x,y), & (x,y) \in \Omega = \left]0, \ell_x\right[\times\left]0, \ell_y\right[, \\ \dfrac{\partial u}{\partial x}(x,0) = g_1(x), & x \in \left]0, \ell_x\right[, \\ u(x,0) = g_2(x), & x \in [0, \ell_x], \\ u(0,y) = h_1(y), & y \in \left]0, \ell_y\right], \\ u(\ell_x, y) = h_2(y), & y \in \left]0, \ell_y\right]. \end{cases} \tag{2}$$

Figure 2 describes the domain considered with the boundary conditions. For these two problems, $g_1(x)$, $g_2(x)$, $h_1(x)$, and $h_2(x)$ are known functions.

The third treated problem is a typical example of an inverse and ill-posed problem of parabolic equation representing the heat phenomena. The problem is given by the following system:

$$\begin{cases} \dfrac{\partial u}{\partial t}(x,t) - a\dfrac{\partial^2 u}{\partial x^2}(x,t) = 0, & \forall (x,t) \in [0,1]\times[x, t_{\text{f}}], \\ u(0,t) = f_0(t), & \forall t \in [0, t_{\text{f}}), \\ u(1,t) = f_1(t), & \forall t \in [0, t_{\text{f}}), \\ u(x, t_{\text{f}}) = g_1(x), & \forall x \in [0,1], \end{cases} \tag{3}$$

where f_0, f_1, and g_1 are functions that describe the boundary and initial conditions, respectively, and t_{f} is a given positive value of the final time and a is a positive number. The boundary temperatures f_0 and f_1 and the final temperature g_1 are known while the initial temperature $u(x,0)$ is unknown and has to be determined. This is usually referred to as the final boundary value problem or the backward heat conduction problem (BHCP). This problem is easily transformed into an initial boundary value problem by a simple variable change. The domain considered with boundary conditions is illustrated in Figure 3.

3. Localized and Space-Time Localized RBF Collocation Method for the Inverse and Ill-Posed Problem

As one of the investigated inverse problems is the time evolutionary partial differential equation, a methodology based on space-time problem formulation is needed. In this section, we describe the space-time problem transformation and localized and space-time localized radial basis function (RBF) collocation methods. The mathematical formulation

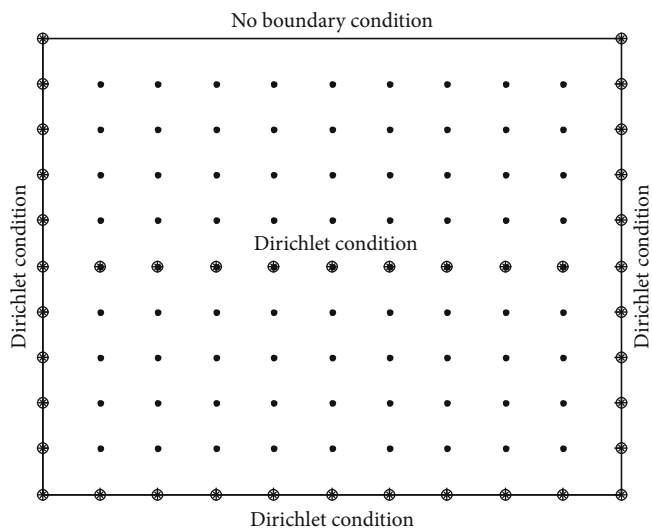

Figure 1: Domain for the first stationary heat problem.

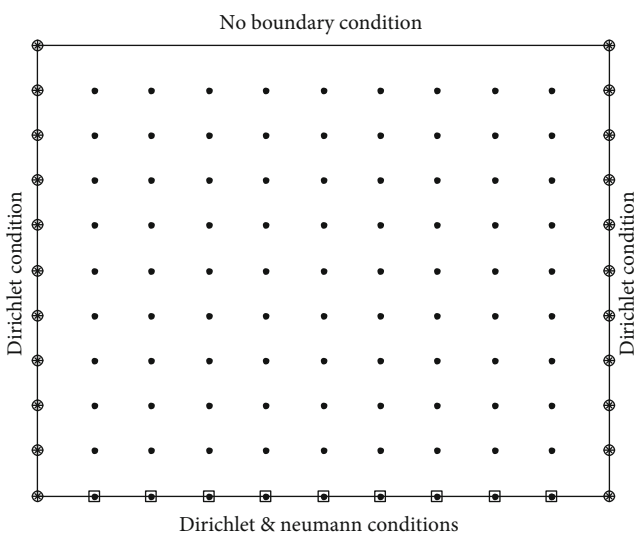

Figure 2: Domains for the second stationary heat problem.

of the two applied methods are the same with respect to the fact that the space-time localized RBF collocation method (ST-LRBFCM) is applied to the evolutionary problem in a space-time domain by combining a space variable and time variable in one vector variable, where the second one, localized radial basis function method (LRBFCM), is applied to the independent time problem defined in the space domain. It can be then remarked that the localized RBF method is just a variant of the space-time localized RBF method. Based on that, only the space-time localized RBF method is reviewed in this section.

3.1. Space-Time Localized RBF Method for the Well-Posed Problem. In the presented formulation, the radial basis function is formulated by taking into account both the spatial and time variables to construct the center points. The d-dimensional space evolving problem is then transformed into a $(d+1)$-dimensional problem and solved in a space-time variable [18]. To apply the technique in the case of a given (BHCP) problem (3) in the space-time domain $\Omega_{t_f} = \Omega \times [0, t_f]$ with a boundary defined by $\partial\Omega \times [0, t_f]$, $\Omega \times \{t = 0\}$, and $\Omega \times \{t = t_f\}$, we require to formulate the boundary conditions of the new formulated system of equations:

$$\frac{\partial u}{\partial t}(x,t) + \mathscr{L}u(x,t) = f(x,t), \tag{4}$$

for the equation in the space-time domain $\Omega \times]0, t_f[$, and

$$\begin{aligned} Bu(x,t) &= g(x,t), \\ u(x,t) &= u_{t_f}(x), \end{aligned} \tag{5}$$

on $\partial\Omega \times [0, t_f]$ and $\Omega \times \{t = t_f\}$, respectively. As the problem is still ill-posed for the space-time domain since it needs a boundary condition on $\Omega \times \{t = 0\}$, Equation (4) can be considered a boundary condition on $\Omega \times \{t = 0\}$.

$$\frac{\partial u}{\partial t}(x,t) + \mathscr{L}u(x,t) = f(x,t) \quad \text{on } \Omega \times \{t = 0\}. \tag{6}$$

The new formulation leads to a complete problem in the space-time variable domain. Then, it can be solved by applying the localized RBFs collocation method described below, which gives us the approximate solution at any point (x, t) (see [18] and the next section for more details).

3.2. Localized RBF Method for the Well-Posed Problem. Let us consider the following boundary value problem:

$$\mathscr{L}u(x) = f(x), \quad x \in \Omega', \tag{7}$$

$$Bu(x) = g(x), \quad x \in \partial\Omega', \tag{8}$$

where $\Omega' = \Omega_{t_f}$ if dealing with the time-dependent problem

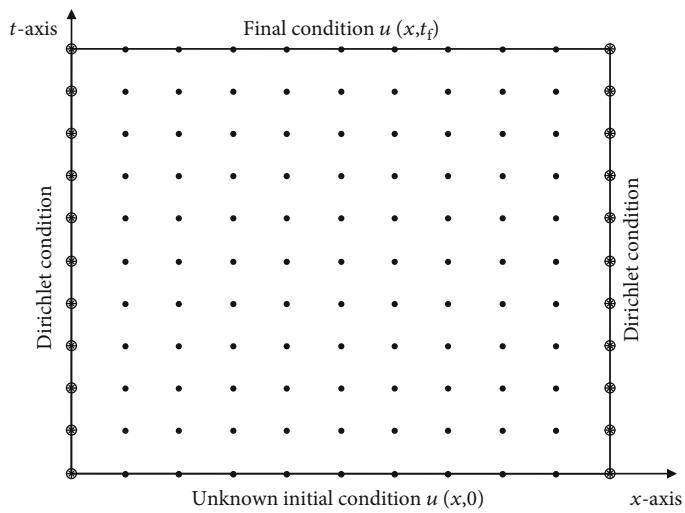

Figure 3: Domain and boundary conditions for the BHCP.

(3) and $\Omega' = \Omega$ in the case of the stationary problem (1) or (2) and $\mathscr{L}$ and B are the given linear domain and boundary differential operators, respectively.

To recall the technique, let $\{x_j\}_{j=1}^{N} \in \Omega' \cup \partial\Omega'$ be center points; for any point $x_s \in \Omega' \cup \partial\Omega'$, a localized influence domain Ω_s is created (see Figure 4). It contains n_s nodal points $\{x_k^{[s]}\}_{k=1}^{n_s}$, including x_s. Following the method of particular solutions (MPS) [20, 21], the solution $u(x_s)$ can be approximated in Ω_s by a linear combination of n_s radial basis functions in the following form:

$$u(x_s) \simeq \widehat{u}(x_s) = \sum_{k=1}^{n_s} \alpha_k \Phi\left(\left\|x_s - x_k^{[s]}\right\|\right), \tag{9}$$

where $\{\alpha_k\}_{k=1}^{n_s}$ are undetermined coefficients and $\|\cdot\|$ is the Euclidean norm. Using Equation (9) and collocating at all $\{x_k^{[s]}\}_{k=1}^{n_s} \subset \Omega_s$, we get the following system:

$$\widehat{\mathbf{u}}^{[s]} = \mathbf{\Phi}^{[s]}\boldsymbol{\alpha}^{[s]}, \tag{10}$$

where $\mathbf{\Phi}^{[s]} = [\Phi(\|x_i^{[s]} - x_j^{[s]}\|)]_{1\le i,j\le n_s}$, $\widehat{\mathbf{u}}^{[s]} = [\widehat{u}(x_1^{[s]}), \cdots, \widehat{u}(x_{n_s}^{[s]})]^T$, and $\boldsymbol{\alpha}^{[s]} = [\alpha_1, \alpha_2, \cdots, \alpha_{n_s}]^T$.From Equation (10), $\boldsymbol{\alpha}^{[s]}$ can be written as follows:

$$\boldsymbol{\alpha}^{[s]} = \left(\mathbf{\Phi}^{[s]}\right)^{-1} \widehat{\mathbf{u}}^{[s]}. \tag{11}$$

For $x_s \in \Omega_s$, we apply the differential operator $\mathscr{L}$ to Equation (9) to obtain the following equation:

$$\mathscr{L}\widehat{u}(x_s) = \sum_{k=1}^{n_s} \alpha_k \mathscr{L}\Phi\left(\left\|x_s - x_k^{[s]}\right\|\right) = [\mathscr{L}\Phi]\boldsymbol{\alpha}^{[s]} = \mathbf{\Lambda}^{[s]}\,\widehat{\mathbf{u}}^{[s]} = \mathbf{\Lambda}\,\widehat{\mathbf{u}}, \tag{12}$$

where $\widehat{\mathbf{u}} = [u(x_1), u(x_2), \cdots, u(x_N)]$ and $\mathbf{\Lambda}^{[s]} = \mathbf{\Theta}^{[s]}\left(\mathbf{\Phi}^{[s]}\right)^{-1}$. Note that by adding zeros at the proper locations based on the mapping of $\widehat{\mathbf{u}}^{[s]}$ to $\widehat{\mathbf{u}}$, $\mathbf{\Lambda}_{1\times N}$ is the global expansion of $\mathbf{\Lambda}_{1\times n_s}^{[s]}$.

Similarly, for $x_s \in \partial\Omega'$, an influence domain Ω_s containing x_s will be created. Then, we have

$$B\widehat{u}(x_s) = \sum_{k=1}^{n_s} \alpha_k B\Phi\left(\left\|x_s - x_k^{[s]}\right\|\right) = B\Phi^{[s]}\,\boldsymbol{\alpha}^{[s]} = \mathbf{\Xi}^{[s]}\,\widehat{\mathbf{u}}^{[s]} = \mathbf{\Xi}\widehat{\mathbf{u}}, \tag{13}$$

where $\mathbf{\Xi}^{s} = B\Phi^{[s]}\left(\mathbf{\Phi}^{[s]}\right)^{-1}$ and $\mathbf{\Xi}$ is the expansion of $\mathbf{\Xi}^{[s]}$ by adding zeros.

By substituting Equation (12) into Equation (7) for $x_s \in \Omega'$ and Equation (13) into Equation (8) for $x_s \in \partial\Omega'$, we obtain the following equations:

$$\begin{aligned} f(x_s) &= \mathscr{L}\widehat{u}(x_s) = \mathbf{\Lambda}(x_s)\widehat{\mathbf{u}}, \\ g(x_s) &= B\widehat{u}(x_s) = \mathbf{\Xi}(x_s)\widehat{\mathbf{u}}. \end{aligned} \tag{14}$$

By collocating all the interpolation points $\{x_j\}_{j=1}^{N}$ using Equation (14), we get the following sparse linear system:

$$\mathscr{M}\mathbf{U} = \mathbf{F}, \tag{15}$$

where

$$\begin{aligned} \mathscr{M} &= \left[\mathbf{\Lambda}(x_1), \mathbf{\Lambda}(x_2), \cdots, \mathbf{\Lambda}\left(x_{N_i}\right), \mathbf{\Xi}\left(x_{N_i+1}\right), \cdots, \mathbf{\Xi}(x_N)\right]^{\mathbf{T}}, \\ \mathbf{U} &= \left[\widehat{u}(x_1), \widehat{u}(x_2), \cdots, \widehat{u}\left(x_{N_i}\right), \widehat{u}\left(x_{N_i+1}\right), \cdots, \widehat{u}(x_N)\right]^{\mathbf{T}}, \\ \mathbf{F} &= \left[f(x_1), f(x_2), \cdots, f\left(x_{N_i}\right), g\left(x_{N_i+1}\right), \cdots, g(x_N)\right]^{\mathbf{T}}. \end{aligned} \tag{16}$$

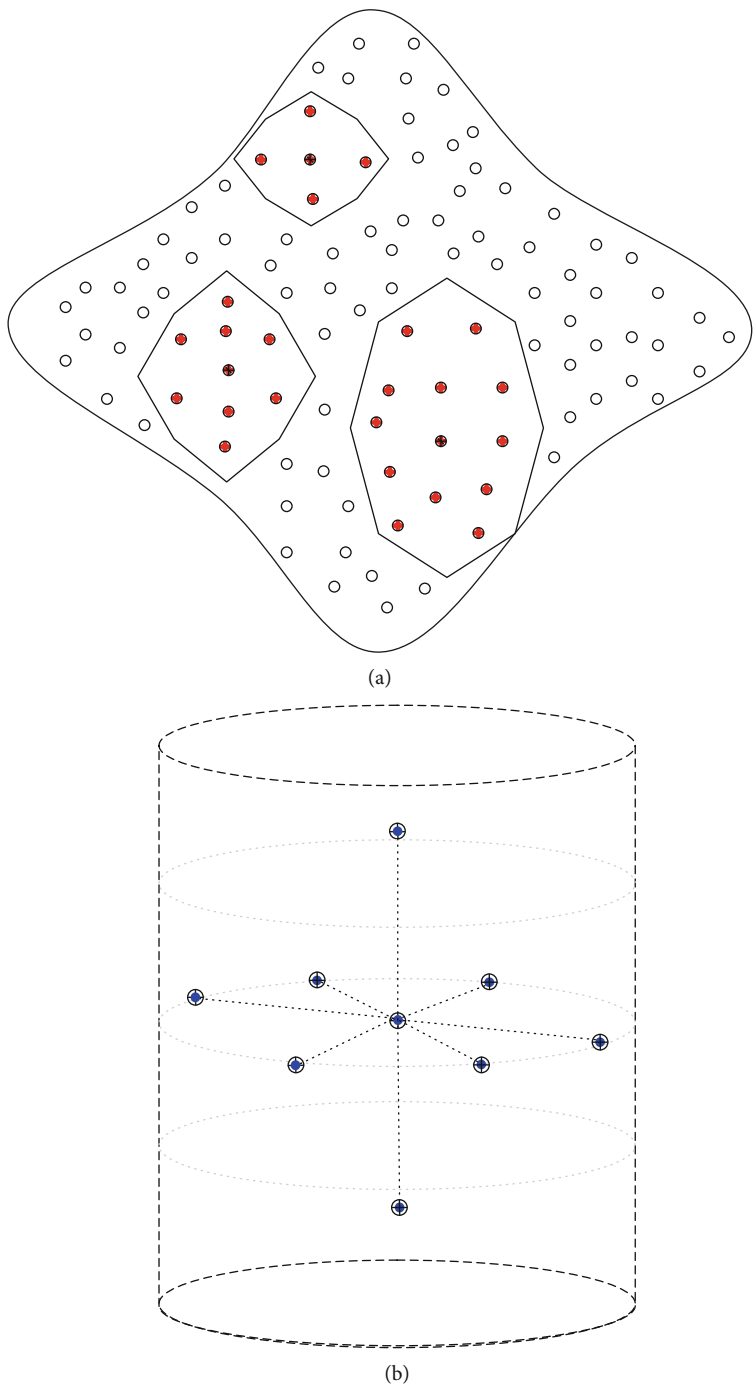

Figure 4: Schematic showing the five-node, nine-node, and thirteen-node local domains Ω_s for 2D (a) and the nine-node local domain for 3D (b).

Note that the linear algebraic system is square since the number of unknowns (the values of the approximate function) and the collocation points are equal. In the next section, the application of such methods to the ill-posed and inverse problem will be demonstrated.

3.3. Localized RBF Method for the Ill-Posed and Inverse Problem. Firstly, we start by explaining the application of the method to the ill-posed problems (1) and (2). As given in the section above, the most important part of these problems is defined by

$$\begin{cases} \Delta u(x,y) = f(x,y), & (x,y) \in \Omega = \left]0, \ell_x\right[\times\left]0, \ell_y\right[, \\ u(x,0) = g_2(x), & x \in [0, \ell_x], \\ u(0,y) = h_1(y), & y \in \left]0, \ell_y\right], \\ u(\ell_x, y) = h_2(y), & y \in \left]0, \ell_y\right]. \end{cases} \tag{17}$$

We can then remark that on the boundary part defined by $]0, \ell_x[\times\{\ell_y\}$, no condition is defined. To solve the problem, more data or boundary condition is needed. For problem (1), potential values at M interior points $u(x_j, y_j)$, $j = 1, \cdots, M$, are given. They are defined by $u(x, \ell_{\text{int}}) = g_1(x)$ in system (1). And, for problem (2), another prescribed boundary condition on the part of the boundary $]0, \ell_x[\times\{0\}$ is given and defined by

$$\frac{\partial u}{\partial x}(x, 0) = g_1(x). \tag{18}$$

Generally, these PDEs have the following form:

$$\begin{cases} \mathscr{L}u(x) = f(x), & x \in \Omega, \\ B_1 u(x) = h_1(x), & x \in \Gamma_1, \\ B_2 u(x) = h_2(x), & x \in \Gamma_2. \end{cases} \tag{19}$$

The domain Ω is a subset of $\mathbb{R}^d$ with a boundary $\partial\Omega = \Gamma_1 \cup \Gamma_3$, $\Gamma_1 \cap \Gamma_3 = \varnothing$. No boundary condition is given on Γ_3. Γ_2 can be a part of $\partial\Omega$ or even $\Gamma_2 \subset \dot{\Omega}$ (interior data). Problem (19) is ill-posed when $\Gamma_2 \subset \Omega$ or $\Gamma_2 \subset \partial\Omega$ and $B_1 \neq B_2$. The operators B_1 and B_2 can be a Dirichlet, Neumann, or mixed boundary condition. B_2 can be the identity operator when h_2 is an interior data.

To solve numerically this problem, we choose N distinct nodes $\{x_j\}_{j=1}^{N} \in \Omega \cup \partial\Omega$ as centers with $N = N_d + N_b$. N_d and N_b are the numbers of centers in Ω and on the boundary $\partial\Omega$, respectively. For the collocation nodes, we take $\{x_j\}_{j=1}^{N_d} \in \Omega$, $\{x_j\}_{j=N_d+1}^{N_1} \in \Gamma_1$, and $N_2 = N - N_1$ nodes $\{x_k\}_k \in \Gamma_2$. Then, we apply (14) to system (19) for each node in Ω or $\partial\Omega$ (depending on the operator used). The obtained algebraic system is square since card (Γ_2) = card (Γ_3) (the number of centers in Γ_3 is equal to the number of collocation nodes in Γ_2). Finally, we get an algebraic system similar to system (15). For the last problem (BHCP), it is solved exactly as shown in Sections 3.1 and 3.2.

4. Numerical Results and Discussions

In this work, we consider two kinds of ill-posed heat problem. The first one, described in Figures 1 and 2, is a two-dimensional stationary heat equation defined by

$$\Delta u(x, y) = 0, \quad (x, y) \in \Omega \subset \mathbb{R}^2, \tag{20}$$

where a condition on a part of the boundary is not known. Two examples of this first type are considered, one with missing boundary condition and internal data and the second with overspecified boundary condition on a part of the boundary.

The second kind of problem is a one-dimensional nonstationary heat problem given by

$$\frac{\partial u}{\partial t}(x, t) - a\frac{\partial^2 u}{\partial x^2}(x, t) = f(x, t), \tag{21}$$

with unknown initial condition. Figure 3 describes the considered example. We should mention that the first problem is solved using the localized RBF method and the second one by the space-time localized RBF method.

Throughout this section, n_s denotes the number of neighboring points in an influence domain for the used localized collocation method. The numbers N_x, N_y, and N_t are the numbers of partitions in each axis used to generate the total number of interpolation points N. The parameter ϵ is either the shape parameter of the well-known multiquadric radial basis function $\varphi(r) = \sqrt{1 + \varepsilon^2 r^2}$ or the inverse multiquadric function $\varphi(r) = 1/\sqrt{1 + \varepsilon^2 r^2}$. The determination of the optimal value of ϵ is still an open subject.

To measure the numerical accuracy, we consider the maximum absolute error (MAE), the root mean squared error (RMSE), and the L^1_{er} relative error defined as follows:

$$\begin{aligned} \text{MAE} &= \max_{1\le j\le N} \left|\widehat{u}(\widehat{x}_j) - u(\widehat{x}_j)\right|, \\ \text{RMSE} &= \sqrt{\frac{1}{N}\sum_{j=1}^{N}\left(\widehat{u}(\widehat{x}_j) - u(\widehat{x}_j)\right)^2}, \\ L^1_{\text{er}} &= \frac{\sum_{j=1}^{N}\left|\widehat{u}(\widehat{x}_j) - u(\widehat{x}_j)\right|}{\sum_{j=1}^{N}\left|u(\widehat{x}_j)\right|}, \end{aligned} \tag{22}$$

where $u(\widehat{x}_j)$ and $\widehat{u}(\widehat{x}_j)$ are the exact and approximate solutions at the node $\widehat{x}_j$, respectively. We consider $\widehat{x}_j = (x_j, y_j)$ for the 2D space examples and $\widehat{x}_j = (x_j, t_j)$ for the BHCP example.

The impact of a number of parameters on the accuracy of the numerical solutions, such as the number of local nodes, the shape parameter of RBFs, and the total number of collocation nodes being used, is also investigated. In the first two examples, we solve the inverse heat problem under the form $\Delta u = 0$ in the two-dimensional domain.

4.1. Problems with Missing Boundary Condition and Internal Data. First, we start by the following ill-posed problem of potential flow investigated by Onishi [22] on a square domain $[0, \ell]^2$. Based on its exact solution given by $u(x, y) = x^2 - y^2$, Dirichlet conditions are prescribed on three sides of the boundary, $u(x, 0) = x^2$, $u(0, y) = -y^2$, and $u(\ell, y) = \ell^2 - y^2$. No boundary condition is given on the fourth side $\{y = \ell\,; 0 < x < l\}$. In the interior, the potential values are known for $y = \ell/2$; $u(x, \ell/2) = x^2 - \ell^2/4$.

We solve the problem without using any boundary condition on $]0, \ell[\times\{y = \ell\}$ and even without collocating the governing equation on its nodal points as it has been done by Cheng and Cabral [12]. So, the algebraic matrix obtained is square. The performance and robustness of this technique will be investigated using the localized RBF collocating method with different radial basis functions such as MQ and IMQ.

To conduct numerical experiments, we take $\ell = 1$ and $n_s = 9$. Tables 1 and 2 show the numerical results obtained for some ϵ, N_x, and N_y using the MQ and IMQ radial basis functions. Figure 5 shows the absolute error of the

Table 1: Errors for example 4.1 for some values of N_x, N_y, and ϵ using MQ.

ϵ	N_x	N_y	MAE	RMSE	L^1_{er}
0.02	11	11	$9.88E-05$	$1.50E-05$	$1.73E-05$
0.04	21	21	$3.37E-04$	$4.34E-05$	$4.45E-05$
0.09	31	31	$4.74E-04$	$5.76E-05$	$7.25E-05$

Table 2: Errors for example 4.1 for some values of N_x, N_y, and ϵ using IMQ.

ϵ	N_x	N_y	MAE	RMSE	L^1_{er}
0.08	11	11	$1.79E-04$	$3.55E-05$	$4.52E-05$
0.02	21	21	$6.19E-04$	$7.73E-05$	$1.02E-04$
0.04	31	31	$2.83E-04$	$2.97E-05$	$4.40E-05$
0.09	41	41	$5.29E-04$	$9.32E-05$	$1.42E-04$

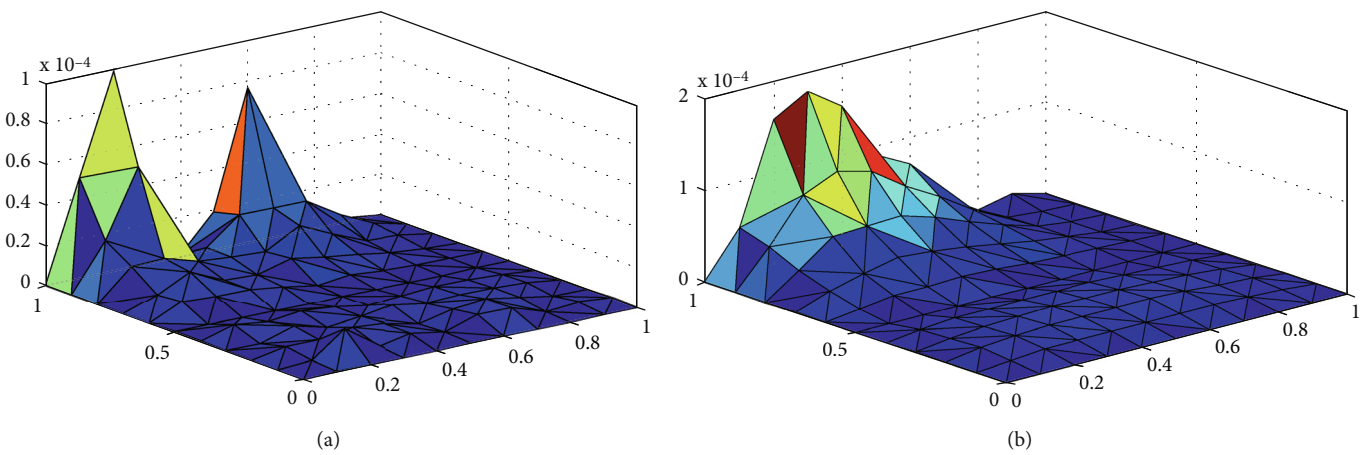

Figure 5: MAE for example 4.1 using MQ with $\epsilon = 0.02$ (a) and IMQ with $\epsilon = 0.08$ (b) with $N = 11 \times 11$.

problem using the MQ function with $\epsilon = 0.02$ and the IMQ function with $\epsilon = 0.08$ and taking $N = N_x \times N_y = 11 \times 11$. It can be remarked that accurate results are obtained in all different cases.

4.2. Problems with Overspecified Boundary Condition. This second ill-posed problem of steady-state heat conduction described below is solved in a square domain $\Omega = [0, 1]^2$ as it was considered by Lesnic [23]. The schematic diagram of the computational square domain is shown in Figure 2. The anticipated exact solution of the problem is $u(x, y) = \cos(x)\cosh(y) + \sin(x)\sinh(y)$. In our situation, we assume that the boundary condition is missing on one side of the domain and the condition of the temperature is prescribed as Dirichlet condition on the three sides of the boundary as $u(x, 0) = \cos(x)$, $u(0, y) = \cosh(y)$, and $u(1, y) = \cos(1)\cosh(y) + \sin(1)\sinh(y)$. To formulate the problem as an ill-posed one, we assume that no boundary condition is given on the fourth part of the boundary described by $\{y = 1\,; 0 < x < 1\}$ and an overspecified Neumann condition is given on the side $\{y = 0\,; 0 < x < 1\}$. For numerical tests, we take $n_s = 9$ and chose different values of ϵ and various numbers of N_x and N_y. Tables 3 and 4 show that accurate results are obtained for different radial basis functions used. Figure 6 depicts the absolute errors in the entire domain of the problem using the MQ with $\epsilon = 0.44$ and the IMQ with $\epsilon = 0.36$ and taking $N = 60 \times 60$ and $N = 50 \times 50$, respectively.

4.3. Backward Heat Conduction Problem (BHCP). In this section, we solve the backward heat condition problem given by Equation (3). This is an example of an ill-posed problem which is difficult to solve using classical numerical methods. This problem has been intensively discussed by Mera et al. [2] and by Jourhmane and Mera [24]. It has been shown in [2] that the matrix of the algebraic system obtained using BEM is severely ill-conditioned. Jourhmane and Mera have then developed an iterative scheme to deal with the ill-conditioning. Their technique is based on a sequence of solutions of well-posed forward heat conduction problems. To discuss the feasibility of our proposed technique, we consider

Table 3: Errors for example 4.2 for different values of N_x, N_y, and ϵ using MQ.

ϵ	N_x	N_y	MAE	RMSE	L^1_{er}
0.11	10	10	$2.98E-03$	$7.07E-04$	$3.36E-04$
0.26	20	20	$1.68E-03$	$2.29E-04$	$7.49E-05$
0.24	30	30	$5.43E-04$	$8.46E-05$	$3.47E-05$
0.55	40	40	$2.12E-03$	$3.50E-04$	$1.22E-04$
0.39	50	50	$1.05E-03$	$1.24E-04$	$3.80E-05$
0.44	60	60	$2.67E-04$	$2.99E-05$	$8.94E-06$

Table 4: Errors for example 4.2 for different values of N_x, N_y, and ϵ using IMQ.

ϵ	N_x	N_y	MAE	RMSE	L^1_{er}
0.10	10	10	$3.64E-03$	$8.81E-04$	$3.92E-04$
0.20	20	20	$5.46E-04$	$1.07E-04$	$5.12E-05$
0.36	30	30	$2.23E-03$	$2.63E-04$	$7.70E-05$
0.43	40	40	$3.19E-03$	$4.59E-04$	$1.42E-04$
0.36	50	50	$6.46E-04$	$9.28E-05$	$3.20E-05$
0.30	60	60	$2.40E-03$	$3.32E-04$	$1.13E-04$

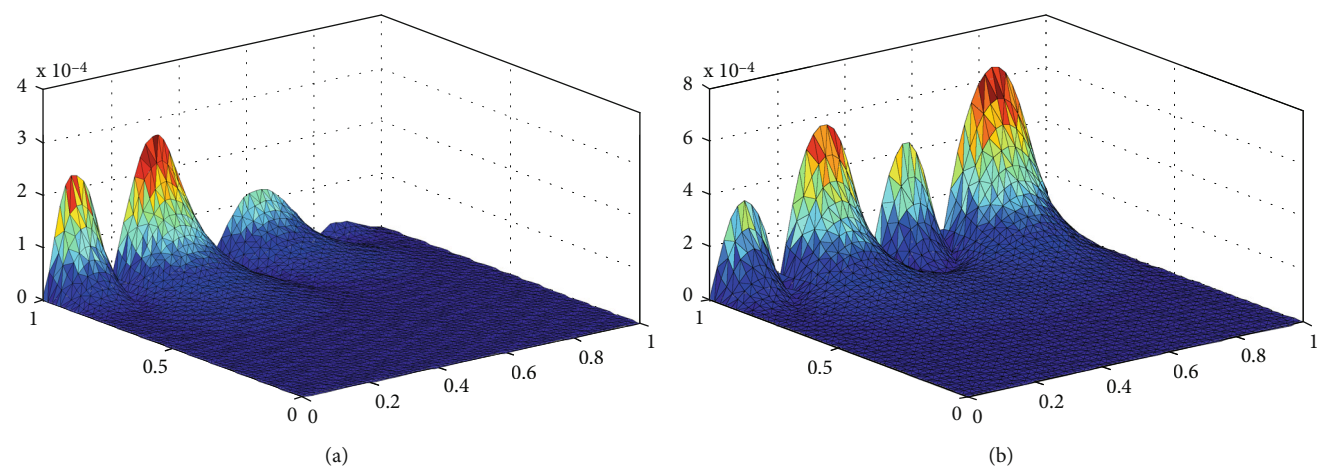

Figure 6: MAE for example 4.2 using MQ with $\epsilon = 0.44$ for $N = 60 \times 60$ (a) and IMQ with $\epsilon = 0.36$ for $N = 50 \times 50$ (b).

the example treated in [2, 23, 24] for which the analytical solution is given by $u(x,t) = \sin(\pi x)e^{-\pi^2 t}$. Following by setting the data f_0 and f_1 to be zero, it can be remarked that for any large t_f, the information given by $g(x) = \sin(\pi x)e^{-\pi^2 t_f}$ are very weak since g approach zero and become smaller than the desired initial condition $u_0(x) = \sin(\pi x)$. Then, the problem shows some difficulties to be solved using some comment techniques. In our case, we show that this problem will be overtaken by using the space-time localized RBF method to solve the problem in the domain $[0,1] \times [0, t_f]$. For this numerical simulation, the obtained results are presented for the MQ-RBF and IMQ-RBF functions and $n_s = 13$. The number of nodes on the x-axis and t-axis are chosen $N_x = N_t = 40$. In Tables 5 and 6, we show the errors obtained at different time t_f and for different values of shape parameter ϵ.

Figure 7 further demonstrates the accuracy of the MAE error at $t = 0$ for $t_f = 1$ and in the entire space-time domain. We remark that even for the big values of t_f such as 0.5, 0.75, and 1, the RMSE is of the order 10^{-4}. It has also been shown that for small values of t_f, the same accurate results are obtained using less than 40 nodes on the t-axis.

4.4. Backward Heat Conduction Problem with Noisy Data. Following Jourhmane and Mera [24], we furthermore investigate the sensitivity of the numerical solution with respect to the noisy boundary data. For that, we assume that the given function g is perturbed by small α and replaced by $g + \alpha$, where α is a Gaussian random variable with mean zero and standard deviation $\sigma = \max|g|(s/100)$. s is the percentage of additive noise included in the input data g. Figure 8 shows

Table 5: Errors for BHCP example 4.3 for different values of t_f using MQ.

t_f	ϵ	MAE	RMSE	L^1_{er}
0.10	0.93	$6.53E-04$	$1.10E-04$	$1.69E-04$
0.20	0.35	$7.90E-04$	$1.77E-04$	$4.69E-04$
0.50	1.255	$5.83E-04$	$7.16E-05$	$1.90E-04$
0.75	1.164	$4.47E-04$	$9.68E-05$	$4.65E-04$
1.00	0.823	$1.59E-03$	$2.73E-04$	$1.62E-03$

Table 6: Errors for BHCP example 4.3 for different values of $t_f$using IMQ.

t_f	ϵ	MAE	RMSE	L^1_{er}
0.10	1.108	$2.25E-04$	$5.98E-05$	$8.85E-05$
0.20	1.073	$2.92E-04$	$7.39E-05$	$1.52E-04$
0.50	1.083	$5.61E-04$	$1.06E-04$	$3.82E-04$
0.75	0.926	$8.62E-04$	$2.09E-04$	$1.18E-03$
1.00	0.913	$2.58E-03$	$3.20E-04$	$1.46E-03$

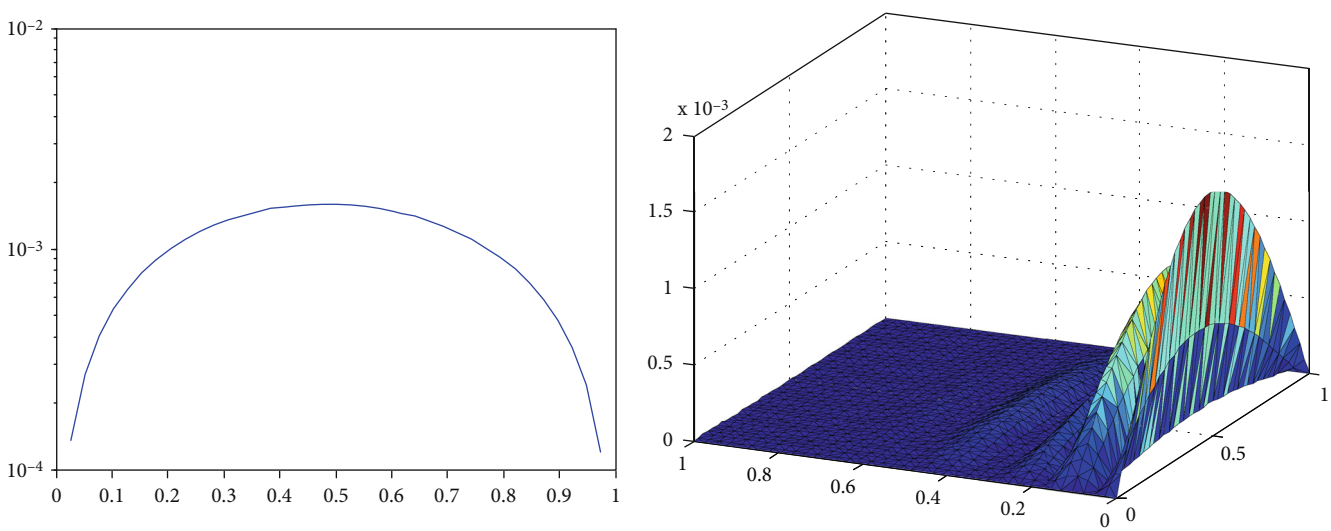

(a) (b)

Figure 7: MAE for example 4.3 using MQ with $\epsilon = 0.823$, $N = 40 \times 40$, and $t_f = 1$.

the numerical obtained approximate solution of initial temperature $u(x, 0)$ for $t_f = 0.1$ and different values of noise $s = 0\%$, 1%, 2%, 3%. From these numerical results, we can mention that as the percentage of additive noise s decreases, the numerical solution approximates better the exact initial solution. The same remark has been declared in [24].

5. Conclusion

In this paper, we presented a localized and space-time localized RBF collocation meshless method to solve the ill-posed and inverse problems in the same way that the well-posed problem is solved and without any iteration method. For the nonstationary problem, we adopted the new space-time localized collocation approach and the problem is solved by the same way as for the localized collocation approach for the stationary case. The results presented show that the method is efficient and gives an alternative of the iteration methods without losing the stability due to iterations. We note that the global RBF method was already used to solve this kind of problem resulting in a rectangular algebraic system [12]. As a further work, we extend the application of the local and space-time local methods for solving the ill-posed problems in higher dimensions and to the nonlinear problems. The numerical algorithms to determinate a good shape parameter will be also investigated.

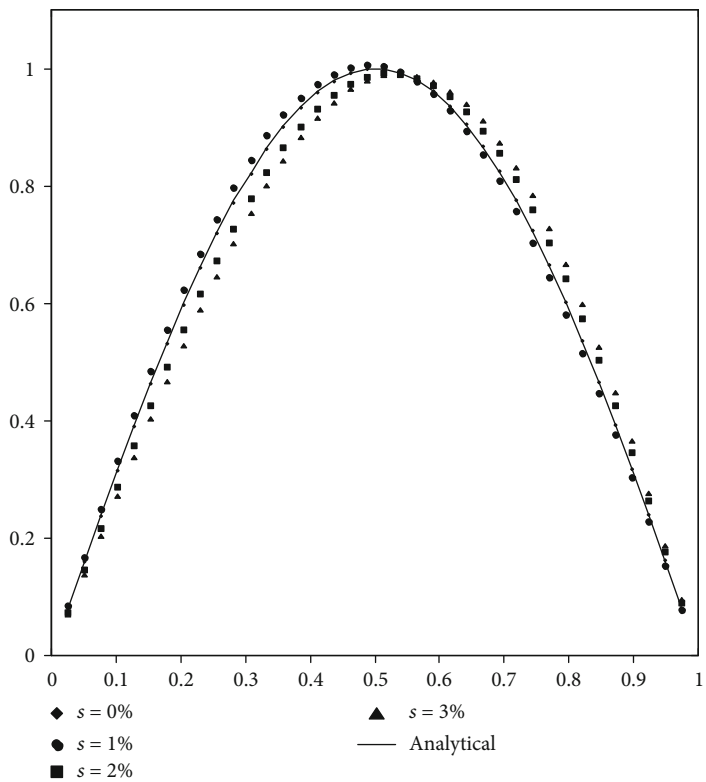

Figure 8: The numerical solution for the initial temperature $u(x, 0)$ obtained for $t_f = 0.1$ with various levels of noise added into the input data for example 4.3.

Data Availability

Data used to support the findings of this study are included within the article.

Conflicts of Interest

The authors declare that there are no conflicts of interest regarding the publication of this paper.

References

[1] V. A. Kozlov and V. G. Maz'ya, "Iterative procedures for solving ill-posed boundary value problems that preserve differential equations," *Leningrad Mathematical Journal*, vol. 5, pp. 1207–1228, 1990.

[2] N. S. Mera, L. Elliott, D. B. Ingham, and D. Lesnic, "An iterative boundary element method for solving the one-dimensional backward heat conduction problem," *International Journal of Heat and Mass Transfer*, vol. 44, no. 10, pp. 1937–1946, 2001.

[3] M. Jourhmane, D. Lesnic, and N. S. Mera, "Relaxation procedures for an iterative algorithm for solving the Cauchy problem for the Laplace equation," *Engineering Analysis with Boundary Elements*, vol. 28, no. 6, pp. 655–665, 2004.

[4] H. Han, D. B. Ingham, and Y. Yuan, "The boundary element method for the solution of the backward heat conduction equation," *Journal of Computational Physics*, vol. 116, no. 2, pp. 292–299, 1995.

[5] N. S. Mera, L. Elliott, and D. B. Ingham, "An inversion method with decreasing regularization for the backward heat conduction problem," *Numerical Heat Transfer, Part B: Fundamentals*, vol. 42, no. 3, pp. 215–230, 2002.

[6] W. B. Muniz, F. M. Ramos, and H. F. de Campos Velho, "Entropy- and Tikhonov-based regularization techniques applied to the backwards heat equation," *Computers & Mathematcs with Applications*, vol. 40, no. 8-9, pp. 1071–1084, 2000.

[7] N. S. Mera, "The method of fundamental solutions for the backward heat conduction problem," *Inverse Problems in Science and Engineering*, vol. 13, no. 1, pp. 65–78, 2017.

[8] Y. C. Hon and M. Li, "A discrepancy principle for the source points location in using the MFS for solving the BHCP," *International Journal of Computational Methods*, vol. 6, no. 2, pp. 181–197, 2011.

[9] C. H. Tsai, D. L. Young, and J. Kolibal, "Numerical solution of three-dimensional backward heat conduction problems by the time evolution method of fundamental solutions," *International Journal of Heat and Mass Transfer*, vol. 54, no. 11-12, pp. 2446–2458, 2011.

[10] Y.-J. Ma, C.-L. Fu, and Y.-X. Zhang, "Solving a backward heat conduction problem by variational method," *Applied Mathematics and Computation*, vol. 219, no. 2, pp. 624–634, 2012.

[11] M. Li, T. S. Jiang, and Y. C. Hon, "A meshless method based on RBFs method for nonhomogeneous backward heat conduction problem," *Engineering Analysis with Boundary Elements*, vol. 34, no. 9, pp. 785–792, 2010.

[12] A. H.-D. Cheng and J. J. S. P. Cabral, "Direct solution of ill-posed boundary value problems by radial basis function collocation method," *International Journal for Numerical Methods in Engineering*, vol. 64, no. 1, pp. 45–64, 2005.

[13] W. Li, X. Liu, and G. Yao, "A local meshless collocation method for solving certain inverse problems," *Engineering Analysis with Boundary Elements*, vol. 57, pp. 9–15, 2015.

[14] Y. Gu, W. Chen, C. Zhang, and X. He, "A meshless singular boundary method for three-dimensional inverse heat conduction problems in general anisotropic media," *International Journal of Heat and Mass Transfer*, vol. 84, pp. 91–102, 2015.

[15] L. Wang, Z. Wang, and Z. Qian, "A meshfree method for inverse wave propagation using collocation and radial basis functions," *Computer Methods in Applied Mechanics and Engineering*, vol. 322, no. 1, pp. 311–350, 2017.

[16] L. Wang, Z. Wang, Z. Qian, Y. Gao, and Y. Zhou, "Direct collocation method for identifying the initial conditions in the inverse wave problem using radial basis functions," *Inverse Problems in Science and Engineering*, vol. 26, no. 12, pp. 1695–1727, 2018.

[17] L. Wang, Z. Qian, Z. Wang, Y. Gao, and Y. Peng, "An efficient radial basis collocation method for the boundary condition identification of the inverse wave problem," *International Journal of Applied Mechanics*, vol. 10, no. 1, article 1850010, p. 26, 2018.

[18] M. Hamaidi, A. Naji, and A. Charafi, "Space–time localized radial basis function collocation method for solving parabolic and hyperbolic equations," *Engineering Analysis with Boundary Elements*, vol. 67, article 152163, pp. 152–163, 2016.

[19] H. Wendland, *Scattered Data Approximation*, Cambridge University Press, 2005.

[20] C. S. Chen, C. M. Fan, and P. H. Wen, "The method of approximate particular solutions for solving certain partial differential equations," *Numerical Methods for Partial Differential Equations*, vol. 28, no. 2, pp. 506–522, 2012.

[21] C. S. Chen, C. M. Fan, and P. H. Wen, "The method of approximate particular solutions for solving elliptic problems with variable coefficients," *International Journal of Computational Methods*, vol. 8, no. 3, pp. 545–559, 2011.

[22] K. Onishi, "Boundary inverse problems in seepage and viscous fluid flows," in *Computer Methods and Water Resources III*, Y. Abousleiman, C. A. Brebbia, A. H.-D. Cheng, and D. Ouazar, Eds., pp. 457–468, Comp. Mech. Publ., 1995.

[23] D. Lesnic, "Inverse initial boundary value problems in heat conduction," *Trends in Heat, Mass & Momentum Transfer*, vol. 4, pp. 37–60, 1998.

[24] M. Jourhmane and N. S. Mera, "An iterative algorithm for the backward heat conduction problem based on variable relaxation factors," *Inverse Problems in Engineering*, vol. 10, no. 4, pp. 293–308, 2002.